Trends in the North Atlantic carbon sink: 1992–2006

David J. Ullman,[1,2] Galen A. McKinley,[1] Val Bennington,[1] and Stephanie Dutkiewicz[3]

Received 17 September 2008; revised 27 May 2009; accepted 26 June 2009; published 24 October 2009.

[1] A biogeochemical general circulation model is used to assess the impact of climate variability from 1992 to 2006 on air-sea CO_2 fluxes and ocean surface pCO_2 in the North Atlantic and to understand trends in the North Atlantic carbon sink over this time period. The model indicates that the North Atlantic carbon sink increased from the mid-1990s to the mid-2000s. Consistent with observations, the model output indicates large changes in the physical and chemical systems of the basin. An analysis of the changes in dissolved inorganic carbon (DIC), alkalinity (ALK), and sea-surface temperature (SST), combined with model-derived DIC tendency terms, allow for an investigation of the mechanisms that dominate the spatial variability and magnitude of the trends in the air-sea fluxes and pCO_2. Modeled parameters compare favorably with available data from the Bermuda Atlantic Time Series in the subtropical gyre and the SURATLANT volunteer observation ship data in the subpolar gyre. Subtropical changes are controlled primarily by changes in sea-surface temperature. Subpolar changes in pCO_2 are instead driven dynamically, primarily through changing vertical supply of DIC. The amplitude of the ocean pCO_2 and air-sea flux trends are largely related to the increase in atmospheric CO_2, but changes to the forcing and circulation of the North Atlantic during this period set the spatial patterns. Model changes are consistent with variation in the North Atlantic Oscillation over the period of study.

Citation: Ullman, D. J., G. A. McKinley, V. Bennington, and S. Dutkiewicz (2009), Trends in the North Atlantic carbon sink: 1992–2006, *Global Biogeochem. Cycles*, *23*, GB4011, doi:10.1029/2008GB003383.

1. Introduction

[2] Since the Industrial Revolution, there has been a marked increase in the concentration of CO_2 in the atmosphere. Human activities, including the burning of fossil fuels, the production of cement, and changes in land use have led to a change in atmospheric CO_2 concentrations from about 280 ppm in 1850 to values of about 380 ppm in 2007 [*Keeling et al.*, 2009]. This increase, however, has been moderated through terrestrial and oceanic sinks that have assimilated roughly half of the total CO_2 emitted from anthropogenic sources [*Solomon et al.*, 2007]. Changes in land use and biomass burning have led to a terrestrial flux of CO_2 from the land to the atmosphere, such that the oceans have served as the only "true" sink for anthropogenic CO_2 over the past 200 years, and were it not for oceanic uptake, atmospheric CO_2 would be 55 ppm higher than present levels [*Sabine et al.*, 2004].

[3] The growth rate of atmospheric CO_2 varies considerably more than estimated anthropogenic CO_2 emissions [*Conway et al.*, 1994; *Peylin et al.*, 2005], indicating that interannual variability of terrestrial and ocean CO_2 sinks are important. Year-to-year changes in climate forcing can have profound impacts on ocean temperature, chemistry, and circulation, all of which impact the ocean carbon cycle [*McKinley et al.*, 2004]. Aside from the prominent role of ENSO variability, the causes of interannual variability in the middle- to high-latitude ocean sink are poorly understood, with estimates of sink magnitudes and variability largely inconsistent from study to study [*McKinley et al.*, 2004; *Gurney et al.*, 2002; *Keeling et al.*, 1996; *Peylin et al.*, 2005; *Baker et al.*, 2006].

[4] There is also significant spatial variability in the ocean sink. Because of differences in ocean circulation and chemistry, each basin has its own inherent ability to absorb atmospheric CO_2. The Atlantic Ocean, in particular the North Atlantic, plays a significant role in the uptake of anthropogenic CO_2. *Takahashi et al.* [2002] estimated that the Atlantic accounts for 41% of the global flux of CO_2 into the ocean. The northern basin comprises only 15% of the global ocean surface, but has absorbed 23% of the anthropogenic carbon stored in the oceans [*Sabine et al.*, 2004].

[5] The main mode of observed physical variability in this region is the North Atlantic Oscillation (NAO) [*Hurrell et al.*, 2003]. During the positive phase of the NAO, an enhanced gradient in surface pressure between the Icelandic Low and Azores High leads to enhanced surface westerly winds over the subpolar gyre associated with a poleward shift in the jet. This leads to deeper mixing and a decrease in sea-surface temperature (SST) in the subpolar gyre, and an increase in

[1]Atmospheric and Oceanic Sciences, University of Wisconsin-Madison, Madison, Wisconsin, USA.
[2]Now at Department of Geoscience, University of Wisconsin-Madison, Madison, Wisconsin, USA.
[3]Earth, Atmospheric, and Planetary Sciences, Massachusetts Institute of Technology, Cambridge, Massachusetts, USA.

0886-6236/09/2008GB003383$12.00

SST in the western subtropics. During a neutral/negative NAO, these circulation anomalies weaken, leading to a subpolar warming and subtropical cooling in SST [*Marshall et al.*, 2001]. *Thomas et al.* [2008] have considered the influence of NAO variability on the North Atlantic surface ocean pCO_2 and CO_2 flux for 1979–2004. They describe separate trends within a positive NAO period in the early 1990s and a neutral NAO in the early 2000s and argue that trends in the ocean carbon sink are heavily influenced by the NAO.

[6] Additionally, significant secular trends in the North Atlantic have been observed over the last few decades. *Schuster and Watson* [2007] and *Schuster et al.* [2009] report on volunteer observation ship (VOS) track data between the Caribbean and the U.K. Along this track, they report a 50% decrease in the sink of atmospheric CO_2 from 1994/95 to 2002/2005 in the northeast area of the section. This may be related to decreasing geostrophic velocity in the subpolar gyre since 1992 [*Häkkinen and Rhines*, 2004]. *Corbière et al.* [2007] similarly report on the reduction of the subpolar sink, with an increase in surface ocean pCO_2 of +2.8 μatm yr^{-1} from 1993 to 2003, related to a strong surface warming of 0.15°C yr^{-1} and a negative shift in the NAO. *Lüger et al.* [2006] report on 2002/2003 VOS data to show that the western sector of the North Atlantic along 34–50°N exhibits a 46% greater sink than the western sector.

[7] In this paper, we use an ocean biogeochemical model to better resolve the physical environment in which these observed carbon cycle changes have occurred. We study the spatial distribution of the changes in the chemical and physical properties of the North Atlantic to better understand the basin's shifting ability to take up CO_2. We consider these changes as "trends" because it has been discussed using this same terminology in the data-based studies to which we compare [*Corbière et al.*, 2007; *Schuster and Watson*, 2007; *Schuster et al.*, 2009; *Thomas et al.*, 2008]. The trends discussed here are limited to the length of the model run (1992–2006) and do not necessarily suggest longer-term tendencies forced anthropogenically or otherwise. Thus, our assessment of variability is limited to intradecadal time scales because of the length of our analysis. A better understanding of multidecadal variability in the North Atlantic carbon cycle requires longer model runs.

2. Methods

2.1. Physical-Biogeochemical-Ecosystem Model

[8] The MIT Ocean General Circulation Model [*Marshall et al.*, 1997a, 1997b] was regionally configured for the North Atlantic between 20°S and 81.5°N, with a horizontal resolution of 0.5° latitude and 0.5° longitude. The model has 23 vertical levels with a resolution of 10 m thickness at the surface increasing to 500 m thickness for depths greater than 2200 m. The Gent-McWilliams [*Gent and McWilliams*, 1990] eddy parameterization and the KPP boundary layer mixing scheme [*Large et al.*, 1994] were employed to represent sub-grid-scale processes. The general circulation model was forced with daily fields from the NCEP/NCAR Reanalysis I [*Kalnay et al.*, 1996] for 1992–2006.

[9] A sponge layer, similar to *Williams et al.* [2006], was included along regional boundaries to dampen the accumulation of tracers in regions that would in reality allow for the flow of tracers to and from other ocean basins. Along the southern boundary, temperature, salinity, dissolved inorganic carbon (DIC), and nutrients were relaxed to climatology. At the Strait of Gibraltar, temperature and salinity alone were relaxed to climatology, as *Béthoux et al.* [1998] suggest that nutrient inflow from the Mediterranean is insignificant. A sponge layer at the northern boundary (north of 81.5°N) was discarded after tests showed that such a sponge layer was inconsequential in this configuration to the regional circulation, temperature, and salinity.

[10] The pelagic ecosystem is parameterized with one zooplankton class and two phytoplankton classes: diatoms and "small" phytoplankton [*Dutkiewicz et al.*, 2005]. Carbonate chemistry is modeled following *Follows et al.* [2006]. The cycling of carbon, alkalinity, phosphorus, silica and iron are explicitly included in the biogeochemical model [*Dutkiewicz et al.*, 2005; *Bennington et al.*, 2009]. Atmospheric pCO_2, including a seasonal cycle, was taken from Mauna Loa observations [*Keeling et al.*, 2009] and is adjusted for local surface atmospheric pressure [*LeQuéré et al.*, 2007; *Doney et al.*, 2007]. The flux of carbon dioxide between the ocean and atmosphere was parameterized following *Wanninkhof* [1992] and with updated coefficients based on the ^{14}C inversion of *Sweeney et al.* [2007]. We define a positive flux as one directed into the ocean.

[11] The physical model was spun up for 81 years while relaxing sponge layer temperature and salinity to monthly climatology (World Ocean Atlas (WOA), *Locarnini et al.* [2006], and *Antonov et al.* [2006]) with time scale of 2 and 4 weeks, respectively. SST was relaxed to 1992–2006 climatological satellite-based estimates [*Reynolds et al.*, 2007], and sea-surface salinity (SSS) was relaxed to WOA surface salinity. After the physical spin up, the biogeochemical model was initialized with GLODAP [*Key et al.*, 2004] DIC and alkalinity (ALK) climatology, WOA nutrients and oxygen [*Garcia et al.*, 2006a, 2006b], low values of phytoplankton and zooplankton, and atmospheric pCO_2 fixed at 356 ppm (roughly the 1992 level). The biogeochemical model was spun up for 70 additional years until all major drift in biogeochemical parameters was eliminated. The results discussed here come from an additional 15-year run using the full biogeochemical model with 1992–2006 NCEP daily forcings, the time-varying atmospheric pCO_2 field, and relaxation to monthly varying SST [*Reynolds et al.*, 2007]. SSS, however, was still relaxed to climatological salinity fields.

[12] To separate the effects on the trends due to changes in climate forcing from the effects on the trends due to anthropogenic increase in atmospheric CO_2, a second run of the model was conducted to assess the effects of the same climate forcings on a carbon system with a constant preindustrial atmospheric CO_2 concentration. Starting from the same physical spin up from above, the biogeochemical model was initialized with GLODAP estimates of preindustrial DIC and ALK climatology [*Key et al.*, 2004] and a constant atmospheric CO_2 of 280 ppm. This was integrated until levels of DIC and ALK stabilized within the model. Once the

carbon and other biogeochemical parameters stabilized, the model was run with the same interannual varying daily NCEP forcings for 1992–2006 with the atmospheric CO_2 remaining fixed at 280 ppm.

2.2. Postsimulation Methods

[13] As described by *Takahashi et al.* [1993], pCO_2 of the surface ocean can be separated into influences from DIC, Temperature (T), ALK, Salinity (S), Phosphate (PO4), and Silicate (SIL) according to the following equation:

$$\frac{dpCO_2}{dt} = \frac{\partial pCO_2}{\partial DIC}\frac{dDIC}{dt} + \frac{\partial pCO_2}{\partial T}\frac{dT}{dt} + \frac{\partial pCO_2}{\partial ALK}\frac{dALK}{dt} + \frac{\partial pCO_2}{\partial S}\frac{dS}{dt} + \frac{\partial pCO_2}{\partial PO_4}\frac{dPO_4}{dt} + \frac{\partial pCO_2}{dSIL}\frac{dSIL}{dt}. \quad (1)$$

Each component was estimated by calculating the pCO_2 with the carbonate chemistry equilibrium constants of the model [*Follows et al.*, 2006; *Mehrbach et al.*, 1973; *Dickson*, 1990, in *Dickson and Goyet*, 1994], using the deseasonalized variability of the component of interest and setting the values of the remaining parameters to their long-term means [*LeQuéré et al.*, 2003; *McKinley et al.*, 2004, 2006]. The sum of each of the components matches reasonably well with the total pCO_2 provided daily model output is used. Across most of the North Atlantic, the change of these pCO_2 components from 1992 to 96 to 2003–06 sum to the total pCO_2 change within 1 μatm, though in a few regions of strong changes, this discrepancy is up to 10 μatm. Salinity, Phosphate, and Silicate represented a small proportion of the overall variability of the total pCO_2 and are therefore excluded from subsequent analysis.

[14] As will be discussed in section 3.4, the model output includes the change in DIC over time due to a number of individual mechanisms driving the DIC concentration. These include effects from vertical mixing, biological uptake, remineralization, freshwater influence (dilution/concentration from precipitation/evaporation), horizontal advection, air-sea flux, and storage (total change over time). We call these tendency terms "DIC diagnostics." The averages of each of these terms was calculated over the top 100m of the model and are used to assess the changes in DIC within a surface layer indicative of a well-mixed surface layer where most of the biological productivity occurs.

3. Results

3.1. Model-Data Comparison

[15] For the most part the physical model compares favorably with the limited observations available in the North Atlantic. Modeled Gulf Stream transports are within 70% of those observed at Cape Hatteras [*Tomczak and Godfrey*, 1994] and in the Florida Strait [*Cunningham et al.*, 2007], as expected for an OGCM of this resolution. Model mixed layer depth (MLD) compared reasonably well with that of WOA climatology, though the model sometimes overestimates maximum winter MLDs at high latitudes. We define the model MLD as the depth where σ_T is different from that of the surface by 0.125 kg/m^3 or more [*Levitus*, 1982]. As shown by *Takahashi et al.* [1993], ocean surface pCO_2 values can be separated into temperature-driven and non-temperature-driven components. *Bennington et al.* [2009] show that modeled seasonal differences of pCO_2 and related temperature and nontemperature components compare favorably with climatological observations [*Takahashi et al.*, 2009]. The model does well in capturing the mean seasonal cycle of pCO_2 and its components [*Bennington et al.*, 2009], a challenging task as illustrated by a recent model and data intercomparison in the North Pacific [*McKinley et al.*, 2006].

[16] A valuable data set for comparing the interannual variability in the data with observations is available from the Bermuda Atlantic Time series Station (BATS, 31°40″N, 64°10″W) [*Bates*, 2007], providing monthly resolved Conductivity-Temperature-Depth (CTD) instrument data and carbon measurements since 1988. The modeled pCO_2 compares favorably with observations in both the timing and magnitude of the pCO_2 cycle (Figure 1a). Similarly, the model captures the SST variability seen in the observations (Figure 1b). Modeled DIC matches the timing of the seasonal cycle (Figure 1c) but underestimates summer DIC drawdown because modeled summertime productivity is too low [*Bennington et al.*, 2009]. Similarly, modeled ALK matches the general observed cycles but does not capture the strong summer reductions (Figure 1d). The insufficient nutrient supply and subsequent insufficient nutrient drawdown causes modeled DIC and ALK drawdowns to be too small. These insufficiencies in DIC/ALK drawdown compensate for each other in their impact on overall pCO_2. In sum, there is a strong correlation between modeled and observed pCO_2, and consistent with observations [*Bates*, 2007], modeled pCO_2 variability at BATS is mostly driven by variability of SST.

[17] From 1993–1997 and 2001–2003, the SURATLANT program collected regular water samples to provide an invaluable data set from the subpolar gyre [*Corbière et al.*, 2007]. The modeled pCO_2, SST, and DIC all compare favorably with the observed data, a combination of *Corbière et al.* [2007] and extension of this work for 2004–2005 (Figures 2a–2c) (N. Metzl, personal communication, 2008), capturing the appropriate magnitudes and important seasonal timing of fluctuations. Modeled ALK (Figure 2d) compares less favorably in terms of the details but still captures the appropriate magnitudes of the mean and variability. Discrepancies in the modeled pCO_2 (Figure 2a) appear to be primarily due to the models inability to fully capture the ALK. The fact that we restore to climatological SSS and do not explicitly model calcifying phytoplankton in the ecosystem is a factor in our ability to fully capture ALK variability.

[18] Such comparisons of modeled data with observations suggest the model is able to capture much of the actual carbon cycle variability in both the subpolar and subtropical gyres. A comparison of modeled and observed trends from the 1990s to the 2000s at each location will be discussed in detail in section 4.

3.2. Temperature Versus Dynamical Controls on Surface pCO_2

[19] The temperature and nontemperature controls on seasonal pCO_2 variability are illustrated in Figures 1 and 2. As discussed in section 3.1, the spatial distribution in these controls on pCO_2 is consistent with climatological observa-

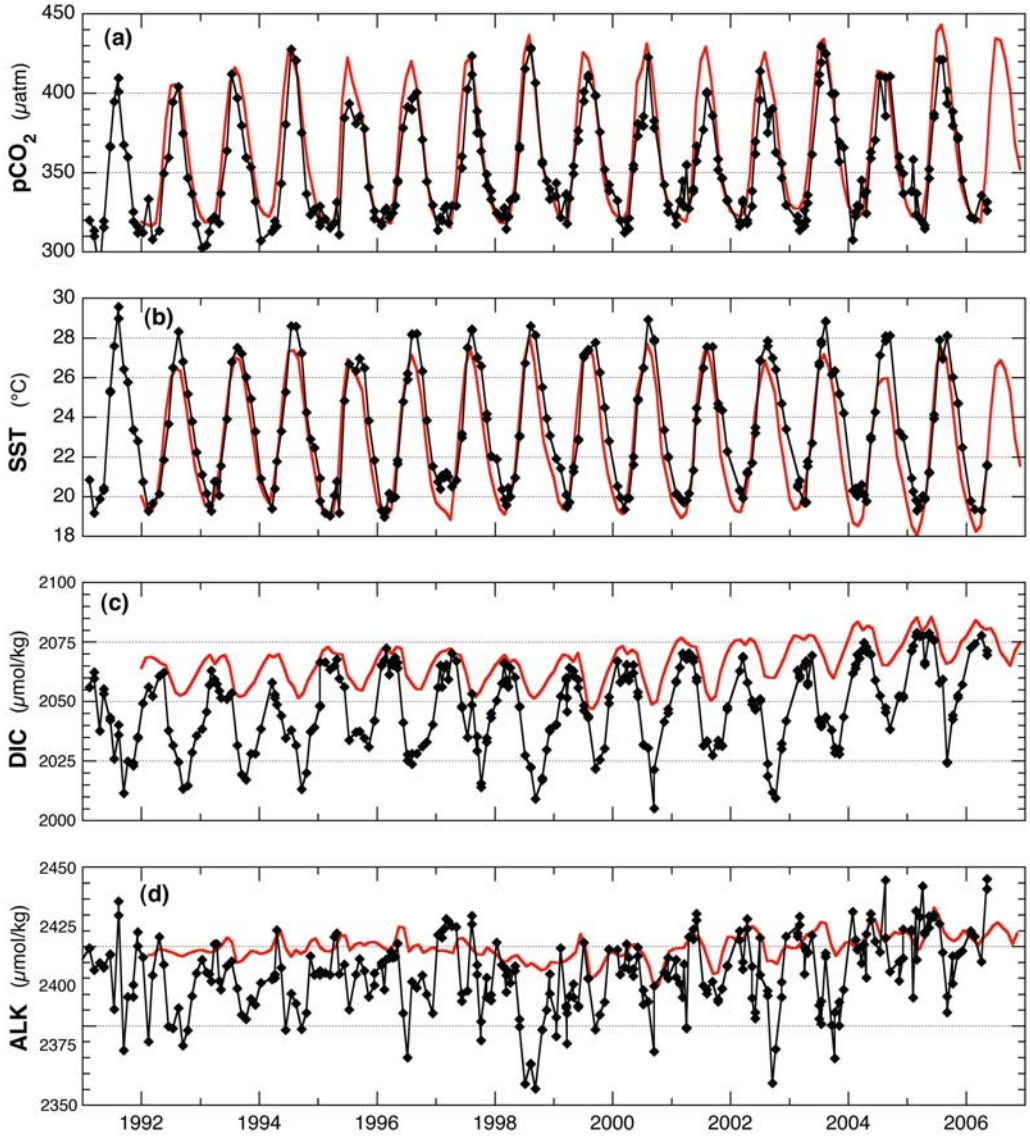

Figure 1. Comparison of (a) pCO_2, (b) sea-surface temperature (SST), (c) dissolved inorganic carbon (DIC), and (d) alkalinity (ALK) between model results and observations at the Bermuda Atlantic Time series Study (BATS)/Hydrostation S from 1983 through 2006 [*Bates*, 2007]. Solid red line indicates model results, while black points represent BATS data with connecting black lines to assist the eye.

tions [*Takahashi et al.*, 2002, 2009]. Consistent with the findings of *LeQuéré et al.* [2003], the two major physical controls on interannual variability in surface ocean pCO_2 are temperature and dynamics, and their effects are typically in opposition. As with the seasonal cycle, interannual pCO_2 variability is dominated by one of these controls (temperature versus dynamics), and this can be seen from the correlation of pCO_2 and SST (Figure 3a). Regions exhibiting a positive correlation are "temperature-driven," such that an increase in SST directly forces an increase in pCO_2 through the thermodynamic controls on gases in seawater. Regions exhibiting a negative correlation between pCO_2 and SST are considered "dynamics-driven," such that anomalous cooling drives additional vertical mixing and DIC supply, which enhances pCO_2. When warming occurs in spring, pCO_2 is reduced due to biological drawdown. As seen in Figure 3a, the dynamics-driven controls on pCO_2 variability are confined to the subpolar gyre, and temperature-driven controls dominate the entire basin south of 45°N.

[20] The subpolar carbon cycle is driven by dynamics, and this is consistent with the deep mixing in this region: the high concentration of DIC mixed to the surface more than offsets the solubility effects due to changes in temperature [*Takahashi et al.*, 2002]. The correlation between pCO_2 and MLD in Figure 3b mirrors that of Figure 3a, showing that the subpolar pCO_2 is indeed positively correlated with deeper mixing [*Lüger et al.*, 2008]. This association shows that vertical mixing is the dominant control on

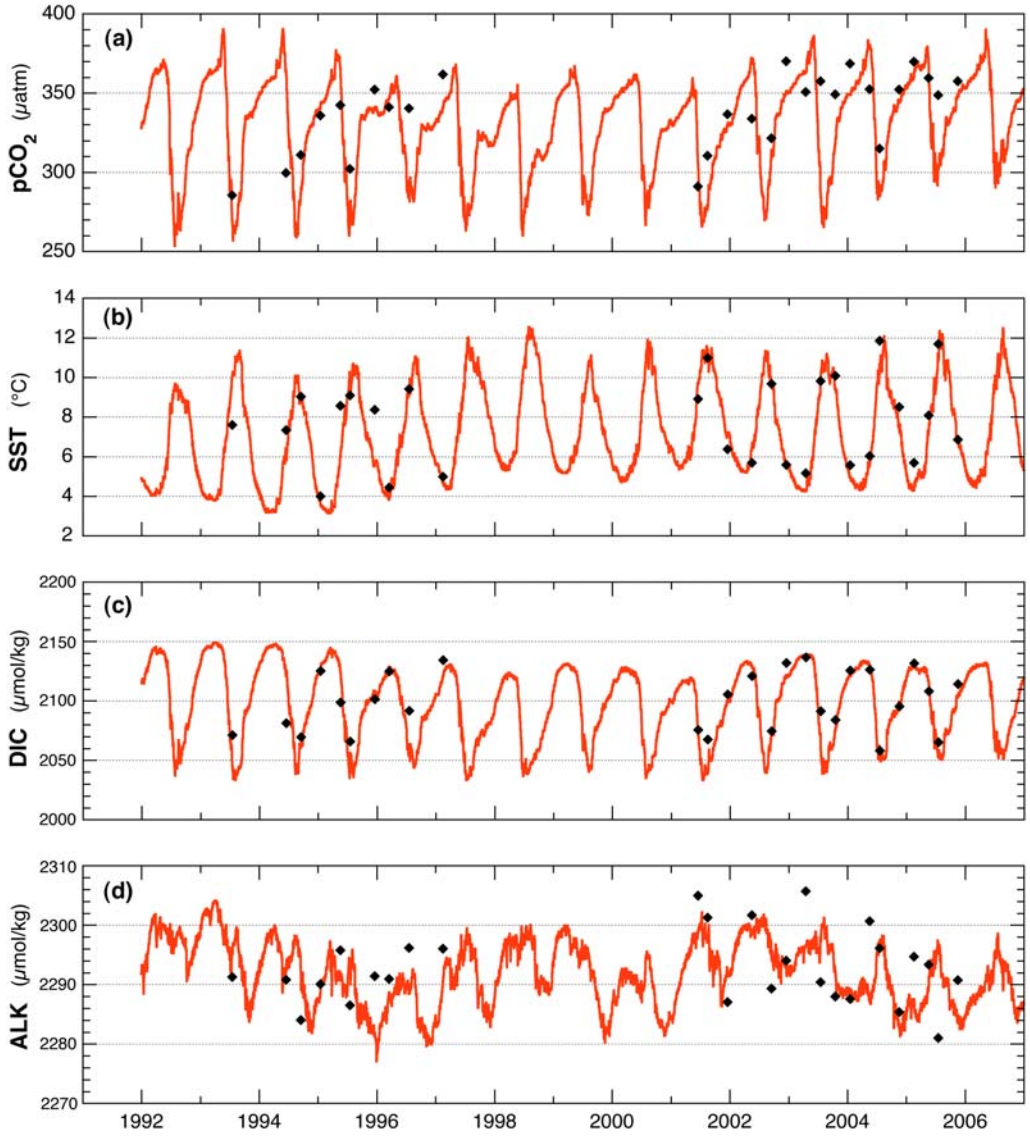

Figure 2. Comparison of (a) pCO_2, (b) SST, (c) DIC, and (d) ALK between model results and observations in the northwest Atlantic Ocean for an area between 45°W and 40°W and 53°N and 57°N. Observational data is from *Corbière et al.* [2007] and A. Corbière et al. (unpublished data, 2004). Solid red line indicates model results, while black points indicate field observations.

pCO_2 in the northern subpolar gyre. The southeastern subpolar gyre (just north of 45°N), however, shows a lack of correlation between pCO_2 and MLD, yet Figure 3a shows that pCO_2 variability is dominated by dynamics and not temperature. Rather than vertical mixing, horizontal transport of DIC may be important to pCO_2 variability in the eastern subpolar gyre, as discussed by *Thomas et al.* [2008]. We further report on the balance of vertical and horizontal processes on surface DIC and pCO_2 in section 4.

3.3. Changes in the Air-Sea CO_2 Flux: 1992–2006

[21] There is a strong increasing trend in North Atlantic air-sea CO_2 fluxes (Figure 4a) from 1992 to 2006. The magnitudes of the modeled regional fluxes are consistent with climatology normalized to 2000 [*Takahashi et al.*, 2009], within the 53% error bars suggested by the authors. There is also substantial interannual variability superimposed onto the increasing trend. The regional CO_2 fluxes from the preindustrial run (thin lines, Figure 4a) shows similar interannual variability to that of the modern run, but the large increasing trend in the modern run is not existent in the flux of the preindustrial run. We conclude that the air-sea flux trend over the 1992–2006 time period is due to the increasing atmospheric CO_2 trend and not to long-term variability in the physical climate or biogeochemistry.

[22] To examine the basin-scale patterns of the temporal change in the CO_2 flux, we consider the difference between 4-year means at the start and end of the run (2003–2006 mean minus 1992–1995 mean). We compare means over 4-year periods to limit the impact of year-to-year variabil-

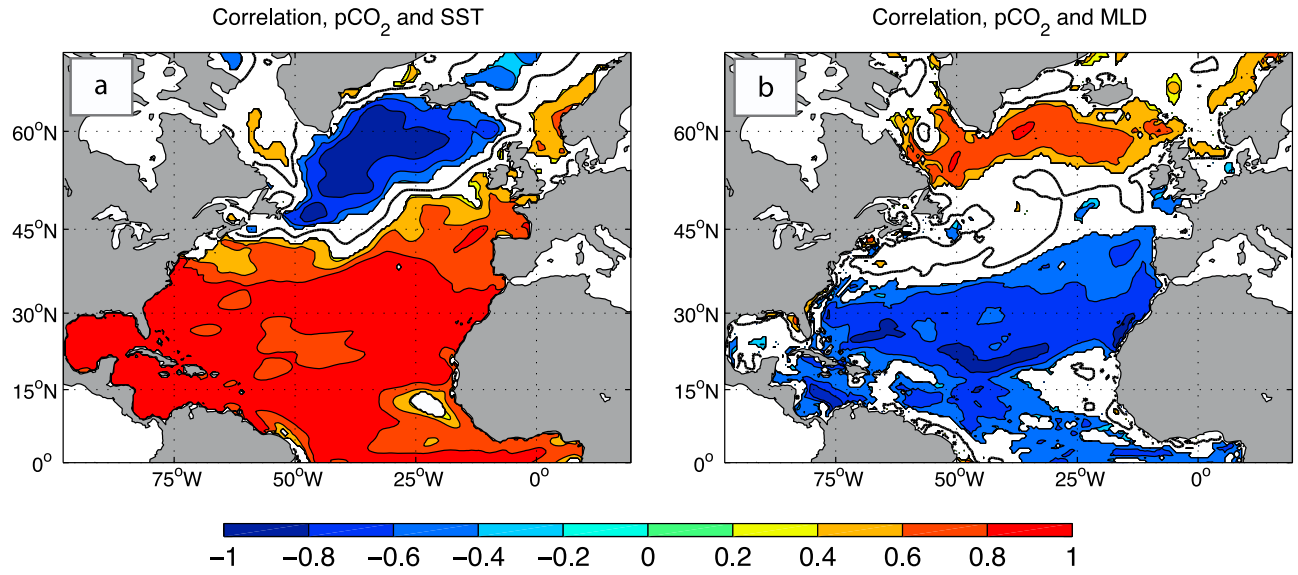

Figure 3. Correlation plots: (a) pCO_2 and SST, (b) pCO_2 and mixed layer depth (MLD). Correlation coefficients were calculated from fields that were detrended and smoothed over 12 months to remove the seasonal cycle. The heavy contour indicates the zero line. White areas indicate those regions where the correlation coefficient is not significantly different from zero at the 95% level.

ity. Different years/lengths for the means were considered and showed the same qualitative results. The choice of these years also allows us to evaluate the impact of the transition from a positive NAO to a neutral NAO on CO_2 fluxes and the related driving mechanisms. Changes in the CO_2 flux (Figure 4b) show a "quad-pole" of four localized centers of action with an increase in the flux in the western North Atlantic (centered at approximately 40°N, 60°W) and in the subpolar gyre south of Greenland (centered at roughly 50°N, 45°W). The air-sea flux shows decreases in the eastern side of the basin, off the coast of the Iberian Peninsula (centered at approximately 45°N, 25°W) and further south in the subtropical gyre (centered at approximately 15°N, 45°W).

[23] To statistically assess the dominant pattern of variability within the modeled carbon system, a principal component analysis (PCA) [*von Storch and Zwiers*, 2002] was conducted on the pCO_2 and CO_2 flux output over 1992–2006. The first empirical orthogonal functions (EOF) of pCO_2 and CO_2 flux explain 73% and 36% of the overall variance, respectively, and both show a strong temporal trend in the first principal component (PC1, Figure 5). At any point in time, the magnitude of the pCO_2 or flux caused by the mode of variability represented by EOF1 is the product of the PC1 and the spatial pattern. Thus, the increasing trend in PC1 indicates that EOF spatial patterns shown in Figures 5a and 5b start out with the opposite phase (since PC1s are negative in 1992), become neutral in about 2000 (when PC1s are zero) and become increasingly positive through 2006. The first EOF of the pCO_2 (Figure 5a) is positive over the entire basin, and the related increase in PC1 indicates that the spatial pattern starts out negative in 1992 and becomes positive and stronger over time. The first EOF of the CO_2 flux (Figure 5b) is positive over the majority of the basin with values up to 0.5 mol m^{-2} yr^{-1} in the subpolar gyre, and some negative values as low as −0.05 mol m^{-2} yr^{-1} (sea to air) in the subtropics extending up along the eastern boundary. These negative regions are collocated with areas of largest positive pCO_2 trend seen in the plot of the first EOF (Figure 5a).

[24] The trends in the PC1 of pCO_2 and the PC1 of the air-sea flux (Figure 5c) are highly correlated (r = 0.87), indicating the expected strong relationship between the variability of the pCO_2 and the flux. The spatial patterns are also similar (Figures 5a and 5b). The high variance explained by each EOF1 and the similarity in patterns between the EOFs and the difference plots (Figure 4b) suggest that a large proportion of the overall changes are driven by the trend. Consistent with *Thomas et al.* [2008], our model results show that the correlation between the first principal component of the pCO_2 and the NAO is weak (r = 0.41). However, we do find a stronger correlation (r = 0.72) between the first principal component of the CO_2 flux and the NAO, indicating that the main mode of variability in the flux is more strongly related to the NAO. Given that the NAO has a strong impact on wind speeds over the North Atlantic and the importance of wind stress on the flux, the stronger association between the flux and NAO variability is not surprising. It should be noted, however, that the NAO only explains 37% of the variance in the winter 500 hPa height [*Marshall et al.*, 2001], suggesting that NAO variability contributes only a portion of the entire climate variability in over the North Atlantic. Given these relationships, we focus on the basin-scale and gyre-scale trends within the context of this shift from positive to neutral NAO.

[25] Because pCO_2 variability is so strongly related to the CO_2 flux variability, we will use pCO_2 to analyze the carbon system over time. The trend in pCO_2 from 1992

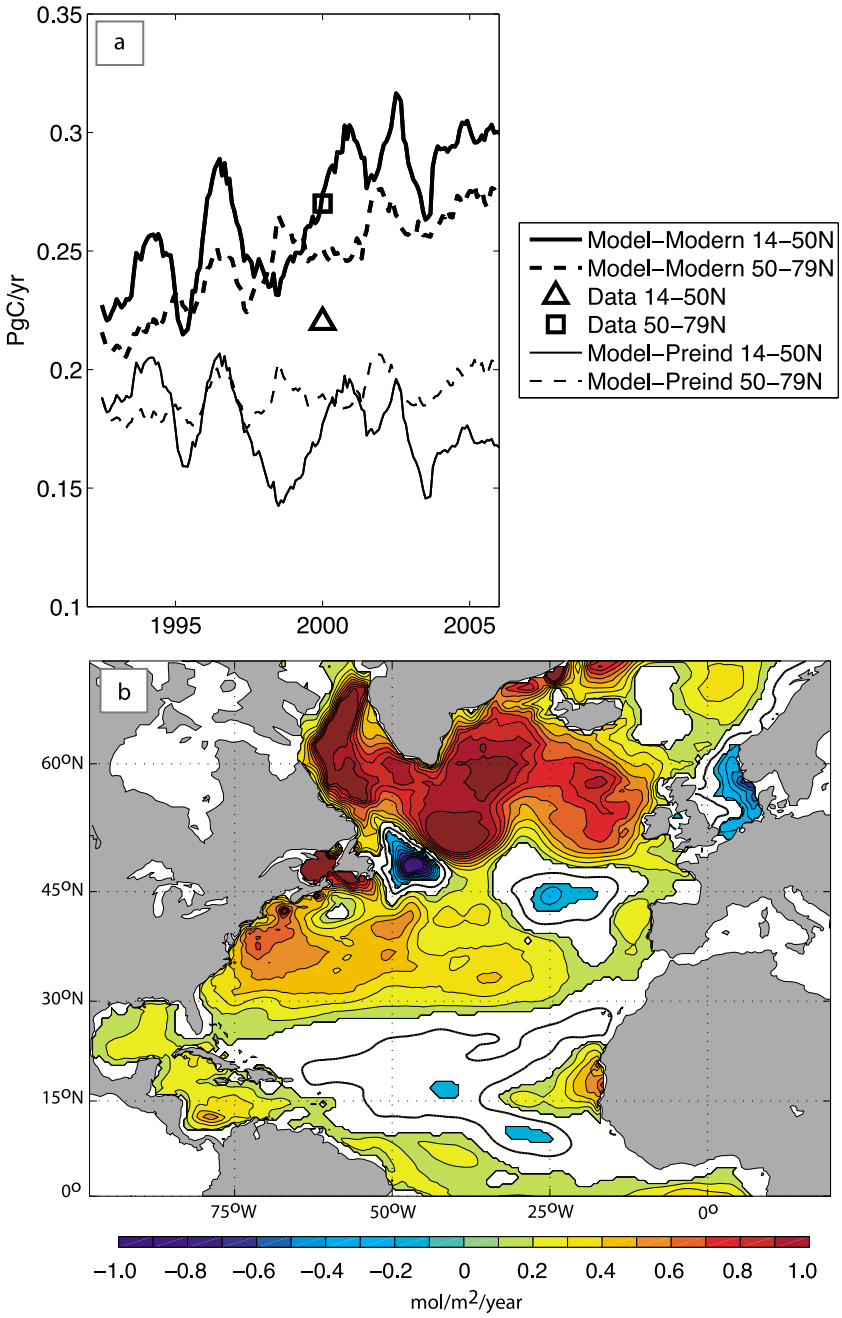

Figure 4. (a) Basin-averaged CO_2 flux for 14–50°N and 50–79°N for modern (bold lines) and preindustrial (thin lines), subpolar (dashed lines) and subtropics (solid lines). Also included on the plot are 2000 observational climatological data points. These data points use *Takahashi et al.* [2009] ΔpCO_2 to calculate the flux using *Wanninkhof* [1992] with updated coefficients from *Sweeney et al.* [2007]. (b) Trend in the CO_2 flux, calculated by taking the difference between the 2003–2006 average and the 1992–1995 average. The heavy contour indicates the zero line. Use of the Mauna Loa time series as the atmospheric pCO_2 boundary condition for all the North Atlantic causes smaller air-sea CO_2 gradients in both summer and winter at high latitudes. Error in the flux estimates due to this is estimated to be, at maximum, 10%.

to 2006 (Figure 6a) shows an increase over the entire basin, driven mostly by the increase in atmospheric pCO_2 (Figure 4a), but this increase is spatially variable, with a quad-pole pattern of lesser/greater increase similar to that described above for Figure 4b. As analyzed in section 3.4, the spatial differences in the magnitude of the ocean pCO_2 increase are related to a number of the factors that influence the chemical balance of carbon in the ocean.

[26] The trends in the pCO_2-ALK, pCO_2-DIC, and pCO_2-SST components (equation (1)) are also shown in Figure 6.

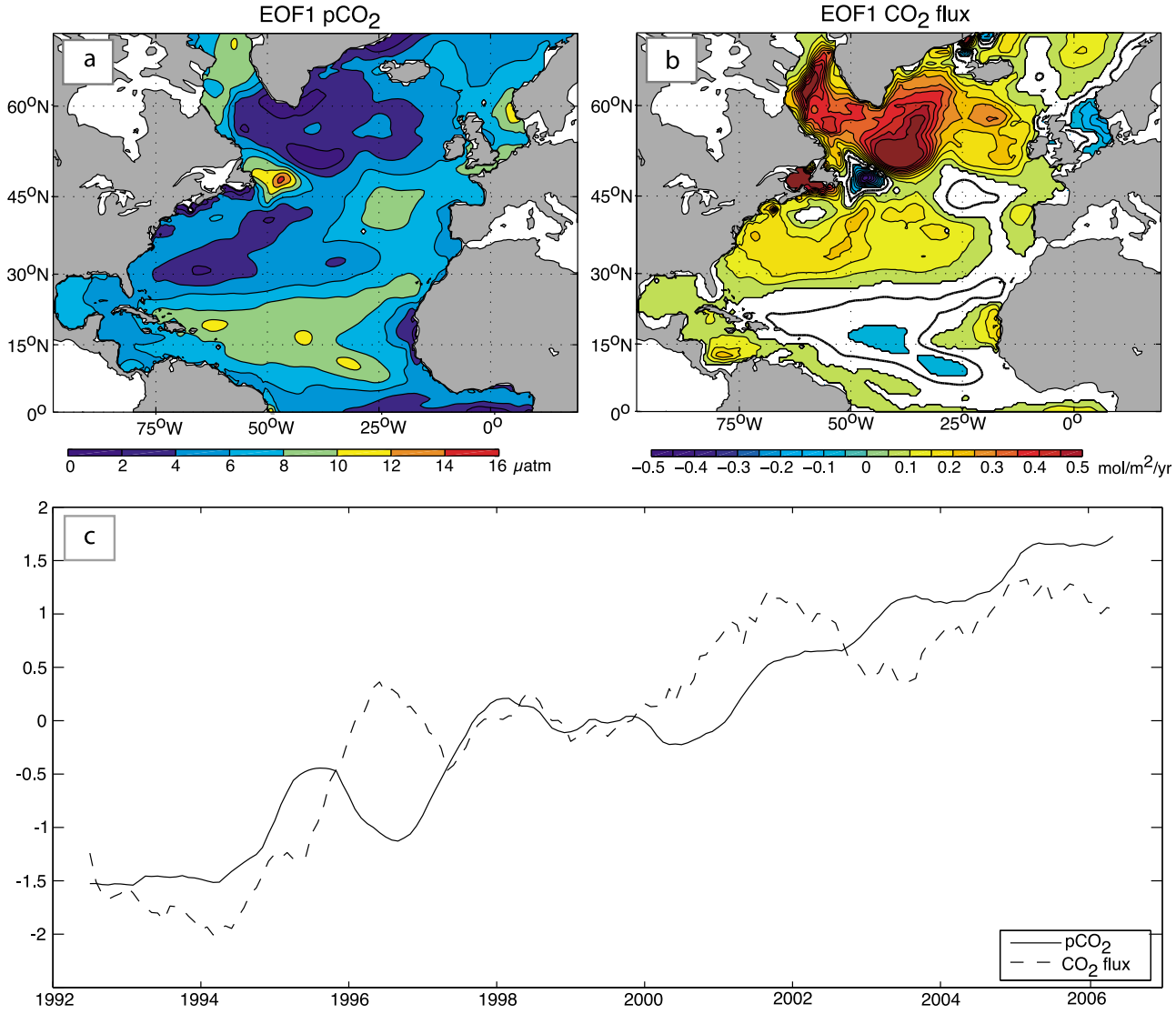

Figure 5. First empirical orthogonal functions of surface (a) pCO_2 and (b) CO_2 flux. The heavy contour indicates the zero line. (c) First standardized principal components of pCO_2 and the CO_2 flux. The two PC1s are highly correlated ($r = 0.87$), suggesting that much of the variability in the air-sea flux of CO_2 is driven by the surface pCO_2.

In the subtropics, the spatial variability of pCO_2 is mostly controlled by variability of SST. In the western subtropical gyre, small increases in overall pCO_2 (Figure 6a) are due to increases in pCO_2-DIC (Figure 6c) but damped by decreases in pCO_2-ALK and pCO_2-SST (Figures 6b and 6d). In the eastern subtropical gyre, where pCO_2-SST is positive, pCO_2 shows a larger increase from 1992 to 2006. However, while the spatial variability in the total pCO_2 trend encompasses much of basin, the highest heterogeneity in the trend of the components is confined to the subpolar gyre. Large increases in pCO_2-ALK and pCO_2-SST are only in part balanced by large decreases in pCO_2-DIC in the subpolar gyre, resulting in only a modest increase in overall pCO_2. This decline in pCO_2-DIC is caused primarily by reduced deep mixing, as discussed in section 3.4. Declining subpolar mixing from 1992 to 2006 also drives changes in alkalinity. With less nutrients coming to the surface, there is a reduction in surface alkalinity, which drives the strong increase in pCO_2-ALK (Figure 6b) in this subpolar gyre. This effect, however, is weaker than pCO_2-DIC changes. Subpolar warming is related to the shift in NAO phase and secular warming during this time period, but we also show a significant change in DIC due to vertical mixing and horizontal advection that compensate the changes in SST (see section 3.4). Though analysis methodologies and the selected time periods differ, these modeled trends in the pCO_2 components are broadly consistent with those found by *Thomas et al.* [2008] for the mid-1990s to the mid-2000s.

[27] The spatial change in pCO_2-SST is highly consistent with observations, including the warming in the Northwest

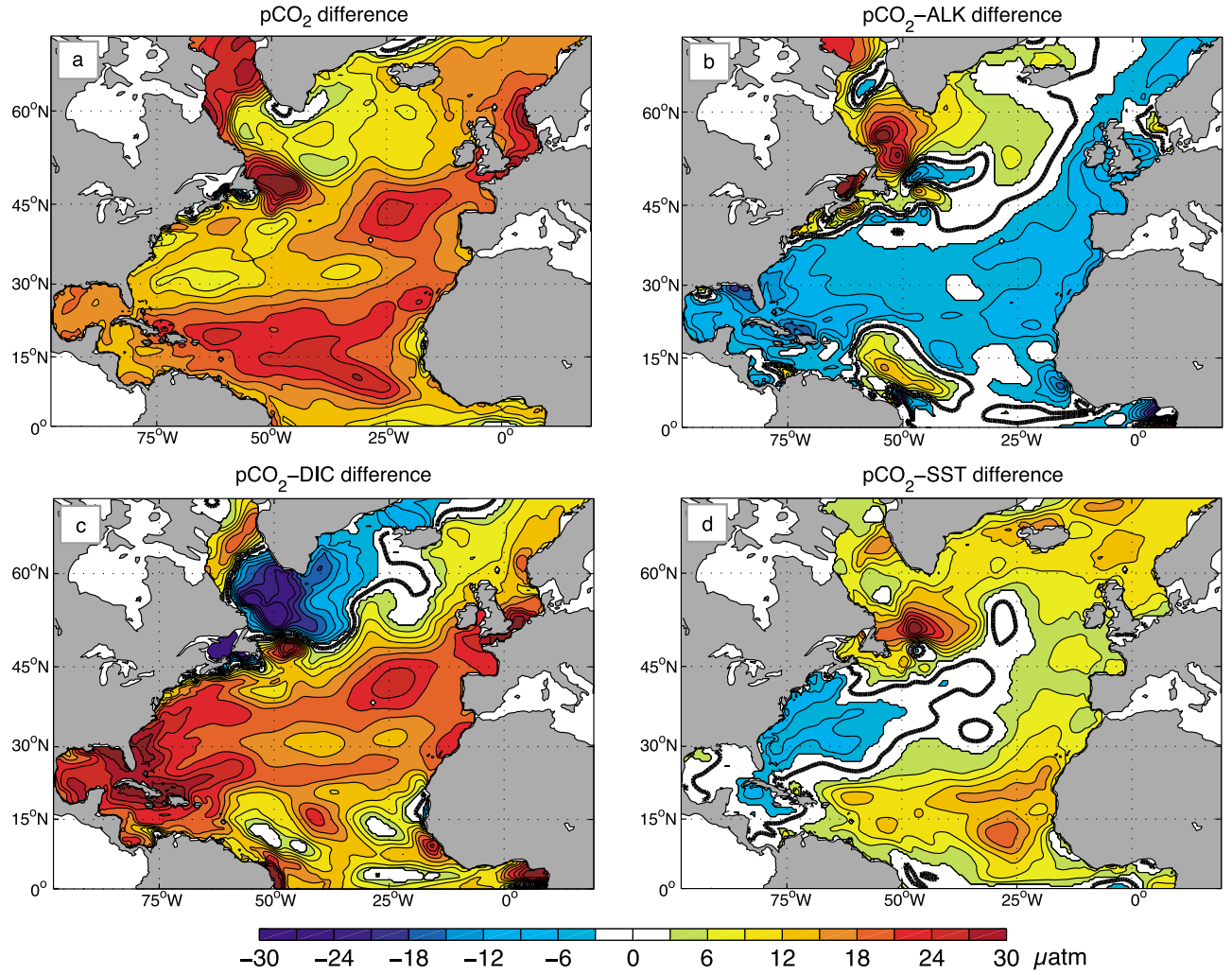

Figure 6. Trend in the (a) pCO_2, (b) pCO_2-ALK, (c) pCO_2-DIC, and (d) pCO_2-SST, calculated by taking the difference between the 2003–2006 averages and the 1992–1995 averages. Areas with values between −3 and 3 μatm have been whited out to accentuate smaller differences around the zero line (heavy contour).

[*Hughes and Holliday*, 2007] from 1992 to 2006. Similarly, satellite data from *Reynolds et al.* [2007] show increased SST north of 50°N over the same time period. These changes in SST have a direct impact on the surface pCO_2, as evidenced from the trend in the pCO_2-SST component (Figure 6d).

3.4. Diagnostics of the DIC Tendency Terms

[28] In section 3.3, we show that DIC changes dominate pCO_2 variability. Model diagnosed DIC tendency terms help to explain the large changes in the subpolar gyre. The mechanistic drivers for DIC change are many, and in this section we use the model to explicitly separate and quantify the contribution from a number of drivers: DIC-vertical, DIC-biology, DIC-fresh, DIC-horizontal, and DIC-flux. Each of these terms quantifies the rate of change in DIC due to each mechanism, described below (units of mmol m^{-3} yr^{-1}). The mean and difference plots of these DIC diagnostic terms, from the two time periods are shown in Figure 7.

[29] DIC-vertical (Figures 7a) quantifies the change in DIC due to vertical advection, diffusion, and all mixing processes. Regions with strong vertical supply of DIC occur along the Gulf Stream and into the subpolar gyre where strong currents and deep mixed layers entrain DIC to the surface. These same regions also show the greatest change from 1992/95 to 2003/06 with a strong decrease in the vertical supply of DIC to the surface. These results are consistent with the decreases in MLD seen in this region (Figure S1a).[1] The largest decrease in MLD occurs in the Labrador Sea and off the southern edge of Greenland and is consistent with observations [*Lazier et al.*, 2002; *Yashayaev*, 2007]. Not surprisingly, shallower MLDs drive a decrease in vertical supply, thus mixing fewer nutrients to the surface (Figure S1b). In the subtropics, DIC vertical supply is rather low, with small or nonexistent changes.

[1] Auxiliary materials are available in the HTML. doi:10.1029/2008GB003383.

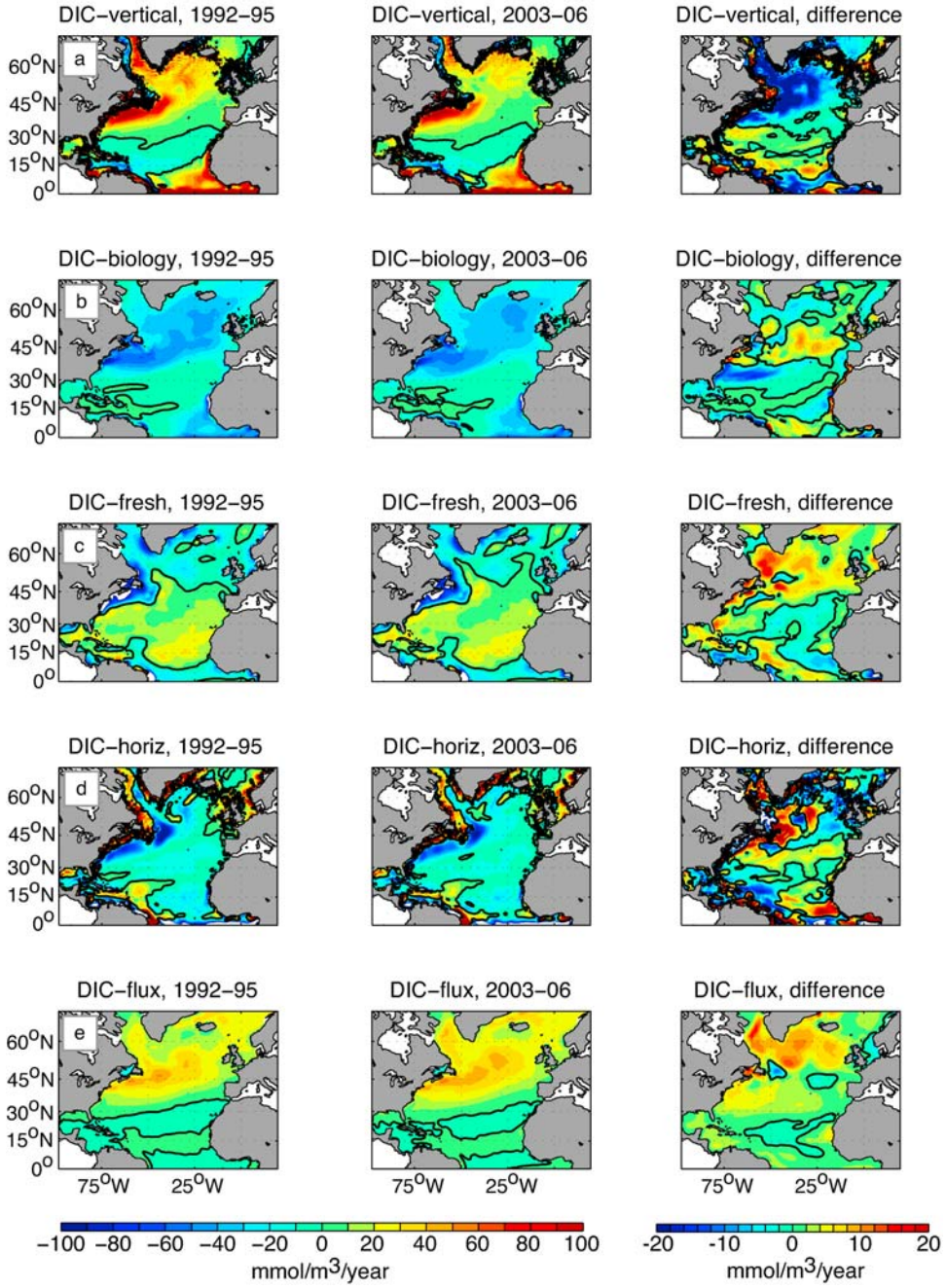

Figure 7. Plots of the DIC Diagnostics: (a) DIC-vertical, (b) DIC-biology, (c) DIC-fresh, (d) DIC-horizontal, and (e) DIC-flux. (left) Mean of values from 1992 to 1995 for each diagnostic. (middle) Mean for 2003–2006. (right) Difference between the two (2003–2006 minus 1992–1995). All diagnostics were calculated using a depth-weighted average over the top 100 m to account for changes that extend below the uppermost 10m, such as biological productivity. The heavy contour indicates the zero line.

[30] DIC-biology (Figures 7b) quantifies the loss of DIC due to uptake of DIC by photosynthesis: negative DIC-biology is indicative of enhanced productivity. Highest biological uptake occurs in subpolar regions. Differences in DIC-biology from 1992/95 to 2003/06 are rather small, with some strong decrease in biological uptake along 45°N. The model also shows some increase in the uptake in the western subtropics along 30°N, which is indicative of a southward shift in the interface between high and low productivity.

[31] DIC-fresh (Figures 7c) quantifies the change in the concentration of DIC due to changes in the input of freshwater: negative DIC-fresh indicates a freshening of surface waters and dilution of DIC. On the mean there is

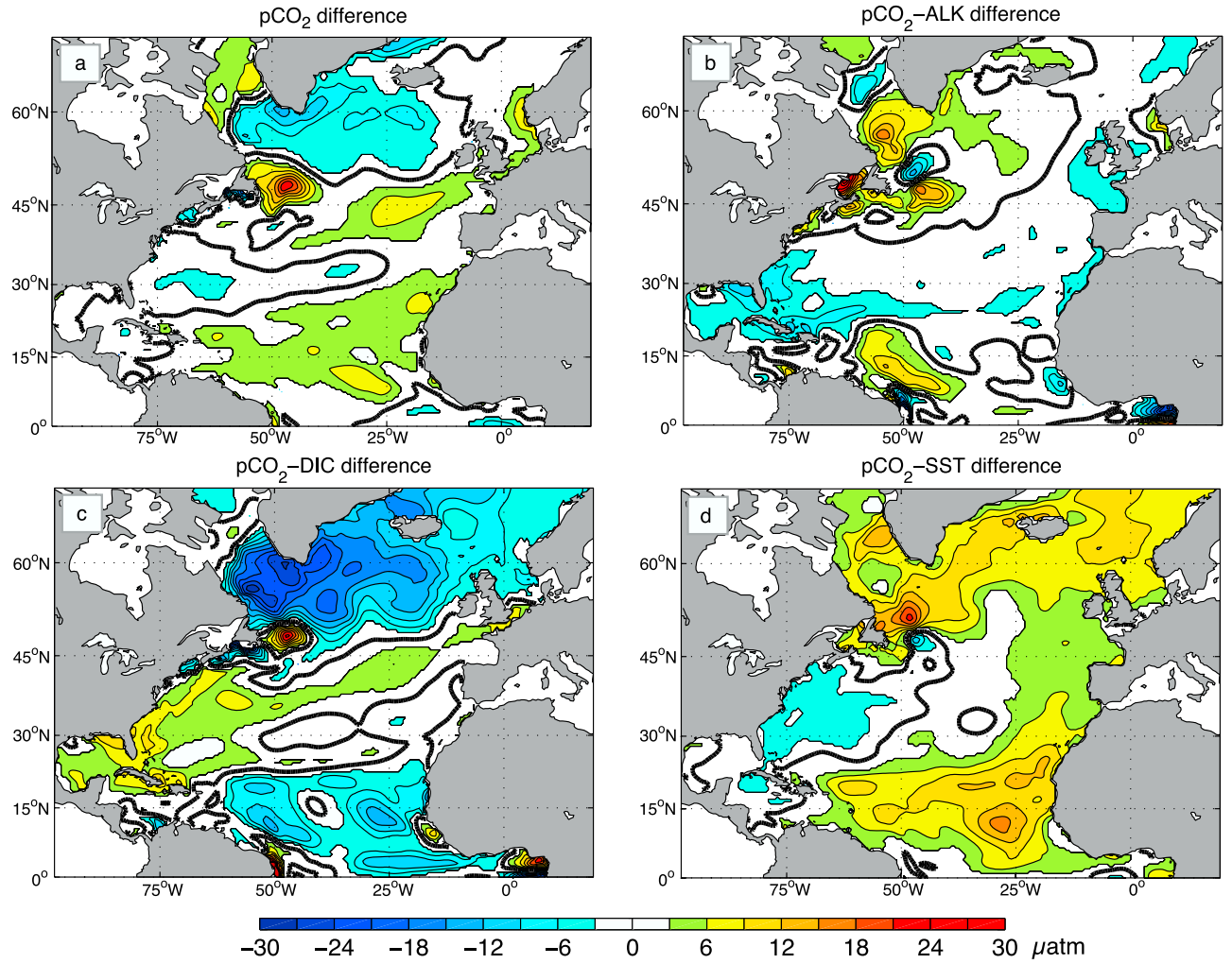

Figure 8. Preindustrial run trends in the (a) pCO_2, (b) pCO_2-ALK, (c) pCO_2-DIC, and (d) pCO_2-SST, calculated by taking the difference between the 2003–2006 averages and the 1992–1995 averages. The heavy contour indicates the zero line.

dilution of DIC (more precipitation than evaporation) in the high north and along the equator, and a concentration (more evaporation than precipitation) elsewhere in the basin. The model shows a concentrating of DIC in the subpolar gyre and Labrador Sea from 1992–1995 to 2003–2006, which is consistent with recent observations of increased salinity in this region [*Hughes and Holliday*, 2007; *Yashayaev*, 2007].

[32] DIC-horizontal (Figure 7d) quantifies the change in DIC due to horizontal advection and diffusion. Not surprisingly, the regions of strongest mean DIC-horizontal occur along the Gulf Stream. The DIC-vertical diagnostic suggests that large amounts of DIC are brought to the surface along the Gulf Stream, but this DIC is rapidly advected out of the region (the strong negative values in DIC-horizontal). Changes in this term in the northeast may be related to changes in the path of the Gulf Stream, consistent with the reduction in subpolar gyre strength over the time period [*Häkkinen and Rhines*, 2004].

[33] DIC-flux (Figure 7e) quantifies the change in DIC due to the air to sea flux. Much of the mean addition of DIC from the air-sea flux is driven by the withdrawal of DIC from the water by biological productivity: the regions of strong DIC-biology and DIC-flux are highly collocated. Trends in the DIC-flux, however, appear to be less related to biological changes and more to changes in the vertical supply. Large subpolar increases in the air-sea flux appear to be driven by the strong decrease of supply of DIC due to vertical processes. The slow rise in atmospheric pCO_2, coupled with the spatial variability of the surface ocean pCO_2 due to combined effects of SST, DIC, and ALK (Figure 6), allows for the air-sea ΔpCO_2 to grow with time (Figure 6a) and thus a significant flux trend to occur.

3.5. Preindustrial Changes

[34] The preindustrial run uses the same interannual climate forcing as the "anthropogenic" run, but without the increasing atmospheric pCO_2. As such, this run helps us identify the changes to pCO_2 and air-sea CO_2 flux that come from circulation changes only. The pCO_2 trend for the preindustrial run (Figure 8a) shows similar spatial patterns, but

considerably lower values than those found in the anthropogenic pCO_2 trend (Figure 6a). The regions in the anthropogenic run that demonstrate less increase in pCO_2 (subpolar gyre, western basin along 30°N) actually show a decrease in pCO_2 for the preindustrial run. This comparison illustrates that natural variability in the climate forcing over the region is driving the spatial variability of the surface pCO_2, consistent with the results of *Thomas et al.* [2008].

[35] While the preindustrial trends in the ALK (Figure 8b) and SST (Figure 8d) are nearly identical to the trends in the anthropogenic run, the preindustrial pCO_2-DIC trend, however, shows a much stronger and broader (spatially) decline in the subpolar gyre. This component is directly connected to the different atmospheric pCO_2 forcing in this run. The preindustrial pCO_2-DIC trend matches the shoaling trend in the MLDs (Figure S1a), confirming that reduced mixing due to changes in climate forcing is driving the decrease in DIC in this region. In the eastern subpolar region of the anthropogenic run, the increased air-sea flux of CO_2, due to the atmospheric pCO_2, compensates for the reduced vertical supply, but this flux is not strong enough to fully compensate in the west.

4. Discussion

[36] In our model study, the pCO_2 trend in the subpolar gyre is largely driven by the changing DIC concentration. Changes in biological productivity, air-sea CO_2 flux, and dilution/concentration by freshwater all alter DIC on a local level to some degree, but changes in horizontal advection and vertical supply have the largest impact in the top 100m (Figure 7). From 1992–1995 to 2003–2006, the model indicates that subpolar DIC decreases are due most dominantly to a reduction in vertical supply. On the basis of a qualitative analysis of temporal changes in observed pCO_2 and its components, *Thomas et al.* [2008] suggest NAO-forced changes in horizontal processes dominate over the North Atlantic pCO_2 variability. However, *Thomas et al.* [2008] do not analyze changes in vertical mixing. Our analysis suggests that although horizontal processes do redistribute DIC, these effects are relatively localized to the southern subpolar gyre. The magnitude of the changes in vertical mixing, however, are larger and dominate the large-scale trends across most of the subpolar gyre, making the total DIC change negative over this period (Figure 6c). Our model indicates that the transition from positive NAO to neutral NAO over 1992–96 to 2002–06 has driven substantial declines in subpolar gyre convection and vertical DIC supply. This has counteracted the impact of the associated warming trend on pCO_2 (Figure 6d), thus allowing for only a small net pCO_2 increase (Figure 6a) and increasing CO_2 sink (Figure 4).

[37] Data available from BATS [*Bates*, 2007] show deseasonalized surface ocean pCO_2, SST, DIC, and ALK increases of 1.20 ± 0.13 μatm yr^{-1}, 0.023 ± 0.008°C yr^{-1}, 1.22 ± 0.08 μmoles kg^{-1} yr^{-1}, and 0.86 ± 0.09 μmoles kg^{-1} yr^{-1}, respectively, calculated for the 1992–2006 period, and applying the errors calculated by *Bates* [2007]. In our model, the changes in pCO_2, SST, DIC, and ALK are 0.81 μatm yr^{-1}, −0.036°C yr^{-1}, 1.09 μmoles kg^{-1} yr^{-1}, and 0.34 μmoles kg^{-1} yr^{-1}, respectively, during the same time period. The DIC trend is only slightly less than observations but the ALK change is too small. The model's restoration to WOA SSS is certainly partially responsible, as relaxation to a climatology will limit ALK trends. Similarly our model SST shows a slight cooling while the observations show a slight warming, and further analysis (not shown) suggests a strong cooling trend in the NCEP heat flux forcing at Bermuda is responsible for this discrepancy. In the overall pCO_2, the reduced model ALK trend is mostly compensated by the DIC, but the reduced SST drives the reduction in the overall model pCO_2 trend as compared to observations.

[38] While the overall magnitude in the modeled western subtropical pCO_2 trend may be low as compared to observations at BATS, the spatial variability captures the tri-pole of subtropical observations in the trend [*Schuster and Watson*, 2007; *Schuster et al.*, 2009] quite well, with larger increases in pCO_2 in the eastern basin, both north and south, separated by smaller increases in the west that extend east over the central subtropics (Figure 6a). This spatial pattern in the subtropics is driven mostly by changes in SST, as seen from the trend in the pCO_2-SST component (Figure 6d), with decreases in the west and increases in the east. The pCO_2-ALK and pCO_2-DIC components (Figures 6b and 6c) oppose each other throughout most of the region, though the DIC component is slightly larger and leads the net increase in pCO_2.

[39] As discussed in section 3.1, the model compares favorably to the data of *Corbière et al.* [2007] across both the 1990s and 2000s in the region 45–40°W, 53–57°N (Figure 2). Detailed analysis indicates that the monthly mean standard error of the model declines between the 1993–97 and 2001–2005 observation periods for pCO_2, SST and DIC, and increases slightly for alkalinity. The fact that the observed alkalinity in the early period of that study was only calculated from SSS is potentially a factor here, but overall, this analysis suggests that the model-data comparison does not degrade over time. Thus, we proceed to a comparison of trends and focus on the wintertime (DJFM) trends from the data, consistent with the analysis by *Corbière et al.* [2007].

[40] Table 1 compares observed and model trends in subpolar pCO_2, SST, DIC, and ALK. Modeled trends in pCO_2 are substantially less than estimated from the relatively sparse observations. The modeled SST wintertime trend is twice that of the DJFM observations. DIC trends in the model show a substantially larger decline than that of the data. ALK trends in the model show a smaller decrease than that of the data. In summary, the trends in this region are substantially different than those estimated from the data, despite the fact that on a point-by-point basis, the model compares well to these same observations (Figure 2).

[41] *Schuster and Watson* [2007] and *Schuster et al.* [2009], using in situ measurements of pCO_2, suggest a spatially varying change in the air-sea flux of CO_2 from the mid-1990s to early-2000s: a decreasing flux in the central subtropical gyre, the eastern subtropics near the Iberian Peninsula, and the western subpolar gyre, and an increasing flux in the western subtropical gyre. While the magnitude of the changes to the air-sea CO_2 flux in the model is smaller than that of those observations, the spatial distribution of the increase/

Table 1. Model and Data Comparison of Parameter Trends in the Subpolar Gyre Region Between 1993 and 1997 and 2001–2005[a]

	pCO_2 (μatm yr^{-1})	SST (°C yr^{-1})	DIC (μmol kg^{-1} yr^{-1})	ALK (μmol kg^{-1} yr^{-1})
		Data		
DJFM trend	2.5[b]	0.09	−0.19[c]	−0.48[d]
Deseasonalized trend[e]	-	-	-	-
		Model		
DJFM trend	0.66	0.16	−0.75	−0.10
Deseasonalized trend[e]	0.87	0.08	−0.32	−0.23

[a]Subpolar gyre region, 45°W to 40°W and 53°N to 57°N. Observational data is from *Corbiere et al.* [2007] and unpublished SURATLANT data (years 2004 and 2005). SST, sea-surface temperature; DIC, dissolved inorganic carbon; ALK, alkalinity.
[b]*Corbière et al.* [2007] report a DJFM pCO_2 trend of 2.8 μatm yr^{-1}, for a larger averaging region and only the period 1993–2003.
[c]*Corbière et al.* [2007] report no trend in DJFM DIC.
[d]Observed ALK was calculated from SSS for 1993–1997.
[e]The deseasonalized (linear least squares) trend is estimated from the time series of daily model results, after removing the mean 1992–2006 seasonal cycle.

decrease is similar to the observations, except in the western subpolar gyre (Figure 4b). *Corbière et al.* [2007] suggest a reduction of the sink in this subpolar gyre region. The limited observations they consider suggest that DIC concentration was relatively constant over the time period, and *Corbière et al.* [2007] argue that the increase in the subpolar pCO_2 is driven by the increase in temperature since the mid-1990s. Our model suggests that while SSTs have indeed warmed, the pCO_2 change has been dominated by a marked decrease in DIC in this region, driven by decreases in mixing and related vertical supply of DIC. Modeled DIC compares well with observations in the subpolar gyre (Figure 2c), clearly capturing the mechanisms governing DIC variability in this region.

[42] In summary, the clearest and largest difference between the model and the data is that the model suggests a substantially greater decline in DIC, even though the model DIC captures the data quite well, particularly in winter (Figure 2c). Though the model's larger increase in SST partially compensates for the DIC change in terms of its effect on pCO_2, the net result is a much smaller positive pCO_2 trend in the model as compared to the observations. With the global atmospheric pCO_2 trend being 1.6 μatm yr^{-1}, the model suggests that the ocean in this region is an increasing sink, while the analysis of the wintertime data alone suggests it is a declining sink [*Corbière et al.*, 2007; *Schuster and Watson*, 2007; *Schuster et al.*, 2009]. The model is, of course, imperfect, but it does have a more complete representation of the temporal evolution of the surface ocean carbon cycle than the relatively sparse observations. We conclude that the strong increase in surface ocean pCO_2 suggested by the data alone is quite possibly an artifact of the temporal sampling and that the smaller trend suggested by the model may be a better representation of the actual behavior of the ocean carbon cycle in this region from the mid-1990s to the mid-2000s.

[43] Decreased mixing in the western subpolar region has also been observed by other studies. Hydrographic observations in the Labrador Sea suggest reductions in MLDs due to a reduction in wintertime convection related to changes in the NAO from positive to neutral phases [*Lazier et al.*, 2002; *Yashayaev*, 2007]. Similarly, *Häkkinen and Rhines* [2004] have reported on a related weakening of the subpolar gyre through the late 1990s related to reduced heat fluxes. Such a spin down of the gyre should lead to a declining slope of the isopycnals and subsequent stratification. An analysis of the changes in the barotropic stream function and tracer release simulations with this model have shown that the model is capturing this weakening of the gyre that is consistent with the decreases in mixing. It is possible that the sparse observations by *Corbière et al.* [2007] did not capture these DIC decreases. However, it is also possible that the model overestimates them.

[44] As an additional point of reference, we consider the trend in this model with respect to the atmospheric inversion of *Rödenbeck* [2005] [see also *Rödenbeck et al.*, 2003; *LeQuéré et al.*, 2007]. Our modeled increase in the CO_2 flux in the subpolar gyres (50–80°N region) goes from 0.22 Pg C yr^{-1} (1993–96 mean) to 0.26 Pg C yr^{-1} (2002–05 mean) for an 18% flux increase. This percent increase is consistent with the atmospheric CO_2 inversion of *Rödenbeck* [2005], who find a 20% flux increase from 0.15 Pg C yr^{-1} to 0.18 Pg C yr^{-1}, respectively, over the same region. This comparison suggests that our model and the inversion are consistent in the direction and relative magnitude of the trend, if not the absolute magnitude of the sinks. The model does suggest that changes in pCO_2 can be localized on the gyre scale, with spatial and temporal heterogeneities making it difficult to extrapolate data to nearby regions or across the basin. The model may be capturing higher spatial/temporal variability not seen in the data [*Corbière et al.*, 2007], given the lower sampling resolution. This analysis is highlighted to stress that the ocean carbon cycle is a four dimensional entity (time included) and that integrating from sparse observations to broad regions may be smoothing over spatial heterogeneities in the carbon system, such as changes due to surface forcing and dynamical transport.

5. Conclusions

[45] We have used a regional ocean biogeochemical model of moderate complexity to assess changes in the carbon sink and other related parameters in the North Atlantic from 1992 to 2006. To a reasonable degree, the model captures the pCO_2 trends observed at BATS [*Bates*,

2007], in the subpolar gyre [*Corbière et al.*, 2007], and along VOS shipping tracks [*Schuster and Watson*, 2007; *Schuster et al.*, 2009]. This model shows that strong, regionally distinct trends in the CO_2 flux and pCO_2 relate to profound change in physical and chemical state of the basin over the 15-year period.

[46] The pCO_2 in the basin south of 45°N is strongly temperature driven. The trends in SST, DIC, and pCO_2 are consistent with BATS time series data and VOS observations. We show that the spatial variability of the pCO_2 trend in this region is primarily driven by SST, but the positive nature of the overall pCO_2 trend across the entire basin occurs from a pCO_2-DIC trend that overcompensates the opposing pCO_2-ALK. DIC diagnostics in this region do not show a clear dominating mechanism. Vertical mixing, biology, freshwater and horizontal transport all contribute to the pCO_2-DIC trends.

[47] We find that the subpolar gyre, however, exhibits dynamics-driven controls on pCO_2, such that changes in vertical mixing have the greatest impact on the overall pCO_2 variability in this region. The modeled pCO_2 is consistent with in situ data (Figure 2a), and model-data discrepancies in pCO_2 are primarily alkalinity driven (Figure 2d). DIC variability, the component that dominates seasonal and interannual variability in pCO_2, is quite well represented (Figure 2c). However, the overall pCO_2 trend from data alone is much larger than in the model, suggesting that the observations may overestimate the trend because of their sparsity. Modeled SST and freshwater changes that drive associated changes in mixing are consistent with hydrographic observations [*Hughes and Holliday*, 2007; *Lazier et al.*, 2002; *Yashayaev*, 2007], suggesting that the model is appropriately capturing some of the major mechanisms in the subpolar gyre, including circulation changes seen in the work of *Häkkinen and Rhines* [2004]. Similarly, an atmospheric inversion [*LeQuéré et al.*, 2007; *Rödenbeck et al.*, 2003; *Rödenbeck*, 2005] suggests an increasing CO_2 uptake in the subpolar gyre over the analysis period that is consistent with the model. Our analysis of the pCO_2 components and the DIC diagnostics of this region show that the modeled decline in pCO_2 in the subpolar gyre over this period is primarily driven by the decrease in vertical supply of DIC, consistent with declining convection as the NAO index has gone from positive to neutral over our analysis period [*Thomas et al.*, 2008]. In this model, the physical forcing that controls mixing is the dominant mechanism of pCO_2 variability, particularly in the western subpolar gyre/Labrador Sea region.

[48] While spatial patterns of pCO_2 change between mid-1990s and mid-2000s appear to be strongly related to variability in climate forcing, the overall magnitude of the trends are driven by the increasing trend in atmospheric CO_2. Results from a preindustrial simulation show that the spatial nature of the changes in pCO_2 and its components is nearly identical to that of the modern simulation, indicating the patterns are driven by the physical forcing and subsequent changes to ocean circulation and mixing.

[49] *Schuster and Watson* [2007] and *Schuster et al.* [2009] argue that there has been a reduction in the carbon sink of $\sim$0.24 Pg C yr^{-1} from the mid-1990s to the early-2000s over a broad area from 20°N to 65°N. The model is not entirely inconsistent with the observations, but it suggests a much smaller increase in surface ocean pCO_2 than the data alone in the western subpolar gyre. We show that any reduction in the sink may be due to a shift in a number of the mechanisms driving the carbon sink such as SST warming and excess DIC accumulation due to circulation and mixing changes. Certainly there has been an increase in atmospheric CO_2 during this time period, and such an increase will drive more CO_2 into the surface ocean, limited by the buffering capacity of seawater (i.e., the Revelle Factor). In a region where the model is consistent with observational data [*Corbière et al.*, 2007], the results of this model show that in the subpolar gyre, surface pCO_2 may have increased much more slowly than the atmosphere. Such discrepancies between the in situ observations and the model highlight the need for further surface carbon observations in this region and neighboring areas to help constrain our knowledge of the magnitude and direction of the flux changes in the subpolar gyre.

[50] Complete time series data (i.e., BATS) has been particularly useful in our understanding of the North Atlantic carbon sink, but this data is limited to the subtropical/temperature-driven regions of the basin. Establishment of a time series in the subpolar/dynamics-driven region of the basin would be invaluable in further assessment of changes in the North Atlantic. Repeat VOS lines [*Schuster and Watson*, 2007; *Schuster et al.*, 2009; *Corbière et al.*, 2007; *Lüger et al.*, 2006] have provided a new source of information about the changing North Atlantic sink that should be continued and expanded. Combined with a need for continued observational data, future modeling work is also needed. In particular, analysis of longer model runs will help to assess longer time scale trends and patterns of variability and further elucidate mechanistic relationships.

[51] **Acknowledgments.** We graciously thank Nick Bates and other scientists and technicians at the BATS site for their data. We are grateful to Nicolas Metzl (LOCEAN/IPSL, CNRS, Paris) and associated CarboOcean partners for assistance with this manuscript and for making unpublished SURATLANT DIC/TA observational data available for our comparisons. We also thank Dierk Polzin for assistance with computing and figures. Funding for this work was provided by NASA (CARBON/04-0300-0228) and the Wisconsin Alumni Research Foundation of the University of Wisconsin-Madison. Stephanie Dutkiewicz also acknowledges the National Science Foundation for funding.

References

Antonov, J. I., R. A. Locarnini, T. P. Boyer, A. V. Mishonov, and H. E. Garcia (2006), *World Ocean Atlas 2005*, vol. 2, *Salinity, NOAA Atlas NESDIS 62*, edited by S. Levitus, 182 pp., U.S. Govt. Print. Off., Washington, D. C.

Baker, D., et al. (2006), TransCom 3 inversion intercomparison: Impact of transport model errors on the interannual variability of regional CO_2 fluxes, 1988–2003, *Global Biogeochem. Cycles*, *20*, GB1002, doi:10.1029/2004GB002439.

Bates, N. R. (2007), Interannual variability of the oceanic CO_2 sink in the subtropical gyre of the North Atlantic Ocean over the last 2 decades, *J. Geophys. Res.*, *112*, C09013, doi:10.1029/2006JC003759.

Bennington, V., G. A. McKinley, S. Dutkiewicz, and D. Ullman (2009), What does chlorophyll variability tell us about export and CO_2 flux variability in the North Atlantic?, *Global Biogeochem. Cycles*, *23*, GB3002, doi:10.1029/2008GB003241.

Béthoux, J. P., P. Morin, C. Chaumery, O. Connan, B. Gentili, and D. Ruiz-Pino (1998), Nutrients in the Mediterranean Sea, mass balance and statistical analysis of concentrations with respect to environmental change, *Mar. Chem.*, *63*, 155–169, doi:10.1016/S0304-4203(98)00059-0.

Conway, T. J., P. P. Tans, L. S. Watermann, K. W. Thoning, D. R. Kitzis, K. A. Masarie, and N. Zhang (1994), Evidence for interannual variability of the carbon cycle from the National Oceanic and Atmospheric Administration/Climate Monitoring and Diagnostics Laboratory Global Air Sampling Network, *J. Geophys. Res.*, *99*, 22,831–22,855, doi:10.1029/94JD01951.

Corbière, A., N. Metzl, G. Reverdin, C. Brunet, and T. Takahashi (2007), Interannual and decadal variability of the oceanic carbon sink in the North Atlantic subpolar gyre, *Tellus, Ser. B*, *59*, 158–178.

Cunningham, S. A., et al. (2007), Temporal variability of the Atlantic meridional overturning circulation at 26.5°N, *Science*, *317*, 935–938, doi:10.1126/science.1141304.

Dickson, A. G. (1990), Standard potential of the reaction: AgCl (s) + 1/2 H2 (g) = Ag (s) + HCl (aq), and the standard acidity constant of the ion HSO_4 in synthetic seawater from 273.15 to 318.15 K, *J. Chem. Thermodyn.*, *22*, 113–127, doi:10.1016/0021-9614(90)90074-Z.

Dickson, A. G., and C. Goyet (Eds.) (1994), *Handbook of Methods for the Analysis of the Various Parameters of the Carbon Dioxide System in Sea Water. (Version 2), ORNL/CDIAC-74*, Oak Ridge Natl. Lab., U.S. Dept. of Energy, Oak Ridge, Tenn.

Doney, S. C., S. Yeager, G. Danabasoglu, W. G. Large, and J. C. McWilliams (2007), Mechanisms governing interannual variability of upper ocean temperature in a global hindcast simulation, *J. Phys. Oceanogr.*, *37*, 1918–1938, doi:10.1175/JPO3089.1.

Dutkiewicz, S., M. J. Follows, and P. Parekh (2005), Interactions of the iron and phosphorus cycles: A three-dimensional model study, *Global Biogeochem. Cycles*, *19*, GB1021, doi:10.1029/2004GB002342.

Follows, M. J., S. Dutkiewicz, and T. Ito (2006), On the solution of the carbonate system in ocean biogeochemistry models, *Ocean Modell.*, *12*, 290–301, doi:10.1016/j.ocemod.2005.05.004.

Garcia, H. E., R. A. Locarnini, T. P. Boyer, and J. I. Antonov (2006a), *World Ocean Atlas 2005*, vol. 3, *Dissolved Oxygen, Apparent Oxygen Utilization, and Oxygen Saturation, NOAA Atlas NESDIS 63*, edited by S. Levitus, 342 pp., U.S. Govt. Print. Off., Washington, D. C.

Garcia, H. E., R. A. Locarnini, T. P. Boyer, and J. I. Antonov (2006b), *World Ocean Atlas 2005*, vol. 4, *Nutrients (Phosphate, Nitrate, Silicate), NOAA Atlas NESDIS 64*, edited by S. Levitus, 396 pp., U.S. Govt. Print. Off., Washington, D. C.

Gent, P. R., and J. C. McWilliams (1990), Isopycnal mixing in ocean general circulation models, *J. Phys. Oceanogr.*, *20*, 150–155, doi:10.1175/1520-0485(1990)020<0150:IMIOCM>2.0.CO;2.

Gurney, K., et al. (2002), Towards robust regional estimates of CO_2 sources and sinks using atmospheric transport models, *Nature*, *415*, 626–630, doi:10.1038/415626a.

Häkkinen, S., and P. B. Rhines (2004), Decline of subpolar North Atlantic circulation during the 1990s, *Science*, *304*, 555–559, doi:10.1126/science.1094917.

Hughes, S. L., and N. P. Holliday (Eds.) (2007), *ICES Report on Ocean Climate 2006, ICES Coop. Res. Rep. 289*, 55 pp., Int. Counc. for the Explor. of the Seas, Copenhagen.

Hurrell, J. W., Y. Kushnir, G. Ottersen, and M. Visbeck (2003), An overview of the North Atlantic Oscillation, in *The North Atlantic Oscillation: Climate Significance and Environmental Impact*, *Geophys. Monogr. Ser.*, vol. 134, edited by J. W. Hurrell et al., pp. 1–35, AGU, Washington, D. C.

Kalnay, E., et al. (1996), The NCEP/NCAR 40-Year Reanalysis Project, *Bull. Am. Meteorol. Soc.*, *77*, 437–471, doi:10.1175/1520-0477(1996)077<0437:TNYRP>2.0.CO;2.

Keeling, R. F., S. C. Piper, and M. Heimann (1996), Global and hemispheric CO_2 sinks deduced from changes in atmospheric O_2 concentration, *Nature*, *381*, 218–221, doi:10.1038/381218a0.

Keeling, R. F., S. C. Piper, A. F. Bollenbacher, and J. S. Walker (2009), Atmospheric CO_2 records from sites in the SIO air sampling network, in *Trends: A Compendium of Data on Global Change*, Carbon Dioxide Inf. Anal. Cent., Oak Ridge Natl. Lab., U.S. Dept. of Energy, Oak Ridge, Tenn., doi:10.3334/CDIAC/atg/035.

Key, R. M., et al. (2004), A global ocean carbon climatology: Results from Global Data Analysis Project (GLODAP), *Global Biogeochem. Cycles*, *18*, GB4031, doi:10.1029/2004GB002247.

Large, W. G., J. C. McWilliams, and S. C. Doney (1994), Oceanic vertical mixing: A review and a model with a nonlocal boundary layer parameterization, *Rev. Geophys.*, *32*, 363–403, doi:10.1029/94RG01872.

Lazier, J., R. Hendry, A. Clarke, I. Yashayaev, and P. Rhines (2002), Convection and restratification in the Labrador Sea, 1990–2000, *Deep Sea Res., Part I*, *49*, 1819–1835, doi:10.1016/S0967-0637(02)00064-X.

LeQuéré, C., O. Aumont, P. Monfray, and J. C. Orr (2003), Propagation of climatic events on ocean stratification, marine biology, and CO_2: Case studies over the 1979–1999 period, *J. Geophys. Res.*, *108*(C12), 3375, doi:10.1029/2001JC000920.

LeQuéré, C., et al. (2007), Saturation of the Southern Ocean CO_2 sink due to recent climate change, *Science*, *316*, 1736–1738.

Levitus, S. (1982), *Climatological Atlas of the World Ocean, NOAA Prof. Paper 13*, 173 pp., U.S. Govt. Print. Off., Washington, D. C.

Locarnini, R. A., A. V. Mishonov, J. I. Antonov, T. P. Boyer, and H. E. Garcia (2006), *World Ocean Atlas 2005*, vol. 1, *Temperature, NOAA Atlas NESDIS 61*, edited by S. Levitus, 182 pp., U.S. Govt. Print. Off., Washington, D. C.

Lüger, H., R. Wanninkhof, D. W. R. Wallace, and A. Körtzinger (2006), CO_2 fluxes in the subtropical and subarctic North Atlantic based on measurements from a volunteer observing ship, *J. Geophys. Res.*, *111*, C06024, doi:10.1029/2005JC003101.

Lüger, H., R. Wanninkhof, A. Olsen, J. Triñanes, T. Johannessen, D. W. R. Wallace, and A. Körtzinger (2008), The sea-air CO_2 flux in the North Atlantic estimated from satellite and ARGO profiling float data, *NOAA Tech. Memo., OAR AOML-96*, 28 pp.

Marshall, J. C., A. Adcroft, C. Hill, L. Perelman, and C. Heisey (1997a), A finite volume, incompressible Navier-Stokes model for studies of the ocean on parallel computers, *J. Geophys. Res.*, *102*, 5753–5766, doi:10.1029/96JC02775.

Marshall, J. C., C. Hill, L. Perelman, and A. Adcroft (1997b), Hydrostatic, quasi-hydrostatic and non-hydrostatic ocean modeling, *J. Geophys. Res.*, *102*, 5733–5752, doi:10.1029/96JC02776.

Marshall, J. C., Y. Kushnir, D. Battisti, P. Chang, A. Czaja, R. Dickson, J. Hurrell, M. McCartney, R. Saravanan, and M. Visbeck (2001), North Atlantic climate variability: Phenomena, impacts and mechanisms, *Int. J. Clim.*, *21*, 1863–1898, doi:10.1002/joc.693.

McKinley, G. A., M. J. Follows, and J. Marshall (2004), Mechanisms of air-sea CO_2 flux variability in the equatorial Pacific and the North Atlantic, *Global Biogeochem. Cycles*, *18*, GB2011, doi:10.1029/2003GB002179.

McKinley, G. A., et al. (2006), North Pacific carbon cycle response to climate variability on seasonal to decadal timescales, *J. Geophys. Res.*, *111*, C07S06, doi:10.1029/2005JC003173.

Mehrbach, C., C. H. Culberson, J. E. Hawley, and R. M. Pytkowicz (1973), Measurement of the apparent dissociation constants of carbonic acid in seawater at atmospheric pressure, *Limnol. Oceanogr.*, *18*, 897–907.

Peylin, P., P. Bousquet, C. Le Quéré, S. Sitch, P. Friedlingstein, G. McKinley, N. Gruber, P. Rayner, and P. Ciais (2005), Multiple constraints on regional CO_2 flux variations over land and oceans, *Global Biogeochem. Cycles*, *19*, GB1011, doi:10.1029/2003GB002214.

Reynolds, R. W., T. M. Smith, C. Liu, D. B. Chelton, K. S. Casey, and M. G. Schlax (2007), Daily high-resolution-blended analyses for sea surface temperature, *J. Clim.*, *20*, 5473–5496, doi:10.1175/2007JCLI1824.1.

Rödenbeck, C. (2005), Estimating CO_2 sources and sinks from atmospheric concentration measurements using a global inversion of atmospheric transport, Tech. Rep. 6, 53 pp., Max-Planck-Inst. for Biogeochem., Jena, Germany.

Rödenbeck, C., S. Houweling, M. Gloor, and M. Heimann (2003), CO_2 flux history 1982–2001 inferred from atmospheric data using a global inversion of atmospheric transport, *Atmos. Chem. Phys.*, *3*, 1919–1964.

Sabine, C. L., R. Feely, Y. Wantanabe, and M. Lamb (2004), Temporal evolution of the North Pacific CO_2 uptake rate, *J. Oceanogr.*, *60*, 5–15, doi:10.1023/B:JOCE.0000038315.23875.ae.

Schuster, U., and A. J. Watson (2007), A variable and decreasing sink for atmospheric CO_2 in the North Atlantic, *J. Geophys. Res.*, *112*, C11006, doi:10.1029/2006JC003941.

Schuster, U., et al. (2009), Trends in North Atlantic sea-surface fCO_2 from 1990 to 2006, *Deep Sea Res., Part II*, *56*, 620–629, doi:10.1016/j.dsr2.2008.12.011.

Solomon, S., D. Qin, and M. Manning (Eds.) (2007), *Climate Change 2007: The Physical Science Basis, Fourth IPCC Report*, Cambridge Univ. Press, Cambridge, U. K.

Sweeney, C., E. Gloor, A. R. Jacobson, R. M. Key, G. McKinley, J. L. Sarmiento, and R. Wanninkhof (2007), Constraining global air-sea gas exchange for CO_2 with recent bomb ^{14}C measurements, *Global Biogeochem. Cycles*, *21*, GB2015, doi:10.1029/2006GB002784.

Takahashi, T., J. Olafsson, J. G. Goddard, D. W. Chipman, and S. Sutherland (1993), Seasonal variation of CO_2 and nutrients in the high-latitude surface oceans: A comparative study, *Global Biogeochem. Cycles*, *7*(4), 843–878, doi:10.1029/93GB02263.

Takahashi, T., et al. (2002), Global sea-air CO_2 flux based on climatological surface ocean pCO_2, and seasonal biological and temperature effects, *Deep Sea Res., Part II*, *49*, 1601–1622, doi:10.1016/S0967-0645(02)00003-6.

Takahashi, T., et al. (2009), Climatological mean and decadal change in surface ocean pCO_2 and net sea-air CO_2 flux over the global oceans, *Deep Sea Res., Part II*, doi:10.1016/j.dsr2.2008.12.009.

Thomas, H., A. E. Prowe, I. D. Lima, S. C. Doney, R. Wanninkhof, R. J. Greatbatch, U. Schuster, and A. Corbière (2008), Changes in the North Atlantic Oscillation influence CO_2 uptake in the North Atlantic over the past two decades, *Global Biogeochem. Cycles*, *22*, GB4027, doi:10.1029/2007GB003167.

Tomczak, M., and J. S. Godfrey (1994), *Regional Oceanography: An Introduction*, 442 pp., Pergamon, Oxford, U. K.

von Storch, H., and F. W. Zwiers (2002), *Statistical Analysis in Climate Research*, 484 pp., Cambridge Univ. Press, Cambridge. U. K.

Wanninkhof, R. (1992), Relationship between wind speed and gas exchange over the ocean, *J. Geophys. Res.*, *97*, 7373–7382, doi:10.1029/92JC00188.

Williams, R. G., V. Roussenov, and M. J. Follows (2006), Induction of nutrients into the mixed layer and maintenance of high latitude productivity, *Global Biogeochem. Cycles*, *20*, GB1016, doi:10.1029/2005GB002586.

Yashayaev, I. (2007), Hydrographic changes in the Labrador Sea, 1960–2005, *Prog. Oceanogr.*, *73*, 242–276, doi:10.1016/j.pocean.2007.04.015.

V. Bennington and G. A. McKinley, Atmospheric and Oceanic Sciences, University of Wisconsin-Madison, 1225 West Dayton Street, Madison, WI 53706, USA.

S. Dutkiewicz, Earth, Atmospheric, and Planetary Sciences, Massachusetts Institute of Technology, 77 Massachusetts Avenue, Cambridge, MA 02139-4307, USA.

D. J. Ullman, Department of Geoscience, University of Wisconsin-Madison, 1215 West Dayton Street, Madison, WI 53706, USA. (ullman@wisc.edu)